UNIVERSITAT POLITÈCNICA DE CATALUNYA
BARCELONATECH

Doctoral School

EMWAVE: A FEM code to simulate wave propagation in magnetically confined plasma domains

Hernán Domingo Ramos

Universitat Politècnica de Catalunya — BarcelonaTech (UPC)
Department of Physics — Ph.D. in Nuclear Engineering and Ionizing radiations

Research plan

August 25, 2025

Directors: Daniel Gallart Escolà
Alejandro Soba Pascual

Tutor: Lluis Batet

Barcelona Supercomputing Center
Centro Nacional de Supercomputación

Contents

1

Introduction to nuclear fusion

In the current state of the global climate crisis, developing a clean, safe, and reliable energy source will be essential for the thriving of humankind. Some green alternatives to conventional fossil fuels are already well known to the general public, such as the broad range of renewable energies—solar, wind, hydroelectric, etc.—or nuclear energy. Despite being excellent substitutes, these solutions still have some drawbacks. For instance, renewable energy is highly dependent on weather conditions, has significant geographic limitations, and often suffers from a mismatch between power generation and grid consumption [1, 2]. On the other hand, the long-term production of radioactive waste and the potential for catastrophic accidents make some groups hesitant about nuclear fission technology.

For these reasons, nuclear fusion has been proposed as a strong candidate for a clean and robust energy source. Fusion offers inherent safety advantages over fission, along with a much higher energy density than uranium and fossil fuels [3]. Consequently, fusion could serve as a green, low-risk, and reliable baseline for energy production.

1.1 Fusion reactions

Thermonuclear fusion reactions occur when two nuclei of light atoms combine. After fusion, the resulting product has a smaller mass than the direct sum of its precursors. According to Einstein's famous formula $E = mc^2$, the energy released in the reaction is given by

$$\Delta E = (m_f - m_i)c^2 \tag{1.1}$$

where the energy in equation eq. (1.1) originates from the mass defect between the reactants and the products. This energy corresponds to the binding energy of the nucleons.

Figure 1.1 provides useful information not only about the physics of fission and fusion energy but also about stellar evolution. To the left of Fe^{56} ($Z = 26$) we find light elements. As a general rule, the lighter the element, the greater the energy produced through fusion. These reactions naturally occur in stellar cores, generating the energy needed to prevent gravitational collapse. Massive stars undergo fusion, forming heavier elements until they reach iron. At that point, fusion can no longer produce energy, leading to the collapse of the outer layers onto the core. On the right side of Fe^{56} in fig. 1.1, heavier elements are found. By fissioning elements such as uranium, lighter elements are produced, releasing energy in the process. This is the operating principle of fission reactors, which use the heaviest elements shown on the right side of fig. 1.1.

There are numerous exothermic nuclear reactions ($\Delta E > 0$, fig. 1.2a), but their reaction rate, which is proportional to the cross-section $\sigma(v)$, depends significantly on the reactants and their temperature, as illustrated in fig. 1.2b. To date, the preferred reaction is the fusion of deuterium ($\mathrm{D} = {}^2_1\mathrm{H}$) and tritium ($\mathrm{T} = {}^3_1\mathrm{H}$), described in eq. (1.2), primarily because it has the highest cross-section at the lowest temperature.

Some alternatives offer certain advantages, such as aneutronic reactions or the use of non-radioactive reactants instead of tritium, but current technology still imposes significant limitations on their feasibility. Achieving aneutronic fusion

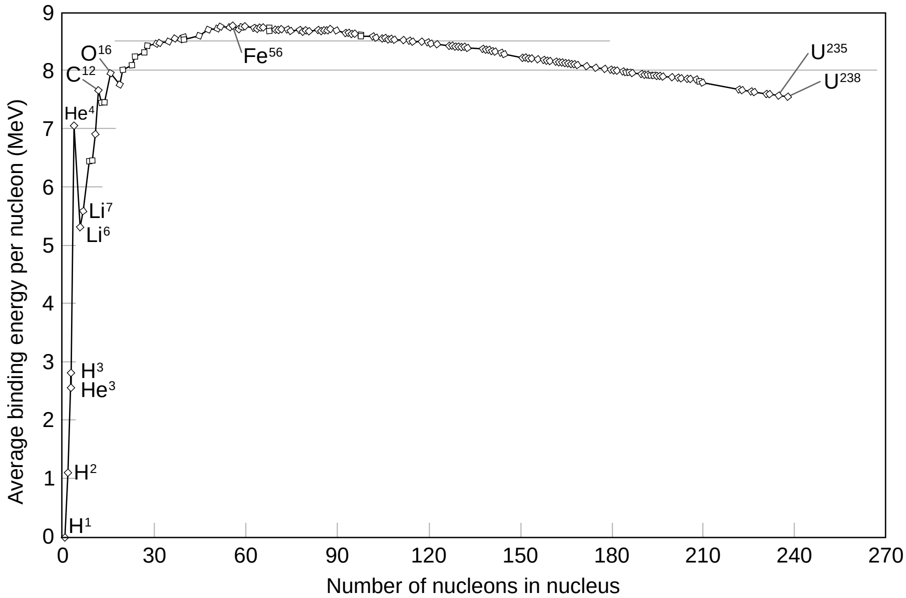

Figure 1.1: Average binding energy of elements. Fe^{56} acts as a limit to exothermic reaction.

would prevent the activation of the reactor wall—thus avoiding the need for high-activation materials such as tungsten—and replacing radioactive fuels like tritium (which has a half-life of just 12.32 years) would allow for larger fuel reserves and eliminate the need for a breeding process inside the reactor.

For tritium breeding to occur, ^{6}Li is required as a seeding material, and current estimates suggest that global ^{6}Li reserves could last for approximately 20 000 years. However, if D + D fusion becomes viable within that timeframe, the vast amount of deuterium present in Earth's oceans could sustain human energy needs for billions of years [3].

$$\mathrm{D} + \mathrm{T} \longrightarrow {}^{4}_{2}\mathrm{He}\,(3.5\,\mathrm{MeV}) + \mathrm{n}\,(14.1\,\mathrm{MeV}) \tag{1.2}$$

1.2 Confinement methods

As seen in fig. 1.2b, the temperature range required to achieve a high cross-section for D-T fusion is on the order of 1.5×10^{8} K (equivalent to ~ 10 keV). At such temperatures, hydrogen isotopes become fully ionized, causing their electrons to separate from their nuclei. This state of free-charged particles is known as plasma.

$$\mathrm{D} + \mathrm{T} \longrightarrow \alpha + \mathrm{n} + 17.6\,\mathrm{MeV}$$
$$\mathrm{D} + \mathrm{D} \longrightarrow {}^{3}\mathrm{He} + \mathrm{n} + 3.27\,\mathrm{MeV}$$
$$\mathrm{D} + \mathrm{D} \longrightarrow \mathrm{T} + \mathrm{p} + 14.05\,\mathrm{MeV}$$
$$\mathrm{D} + {}^{3}\mathrm{He} \longrightarrow \alpha + \mathrm{p} + 18.34\,\mathrm{MeV}$$
$$\mathrm{D} + {}^{6}\mathrm{Li} \longrightarrow 2\,\alpha + 22.4\,\mathrm{MeV}$$
$$\mathrm{D} + {}^{7}\mathrm{Li} \longrightarrow 2\,\alpha + 17.2\,\mathrm{MeV}$$
$$\mathrm{D} + {}^{6}\mathrm{Li} \longrightarrow \alpha + {}^{3}\mathrm{He} + 4.0\,\mathrm{MeV}$$
$$\mathrm{D} + {}^{11}\mathrm{Be} \longrightarrow 3\,\alpha + 8.7\,\mathrm{MeV}$$

(a) Examples of nuclear fusion reactions [4].

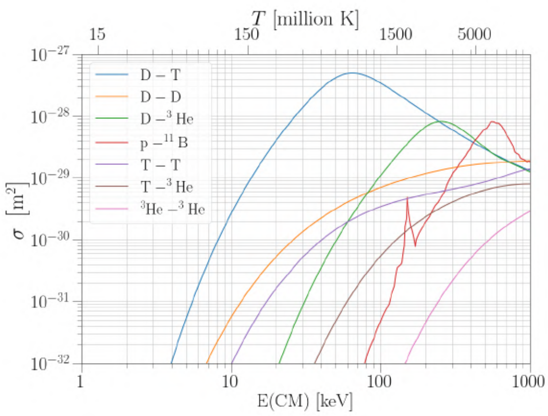

(b) Cross-section for some of the reactions. Data extracted from [5, 6].

Figure 1.2: Some reactions present different advantages, but the easiest to achieve is D + T.

To prevent the hot material from coming into contact with the reactor walls and to improve heating efficiency, the plasma must be confined within a limited region.

The two most relevant approaches to achieving fusion energy are magnetic confinement and inertial confinement. Inertial confinement fusion (ICF) is a fusion energy research method that seeks to initiate nuclear fusion reactions by heating and compressing a fuel target, typically a small pellet containing a mixture of deuterium and tritium [7]. In this process, a laser or ion beam is directed at the pellet, causing the outer layer to evaporate due to the enormous energy influx. This results in energetic collisions that drive part of the pellet inward, dramatically increasing the density of the inner core—by a factor of a thousand—and raising its temperature to the ignition point for fusion. This must occur within a time interval of 10^{-11} to 10^{-9} seconds, which is too short for the ions to move significantly due to their own inertia; hence the term *inertial confinement*.

On the other hand, magnetic confinement takes advantage of the high conductivity of plasma, as its charged particles move independently. When a magnetic field is applied, the motion of these charges is constrained to a circular motion in the perpendicular plane to the magnetic field. If the particle also has a velocity component along the magnetic field direction, its resulting motion will be helicoidal. Mathematically, this is expressed as:

$$\vec{z} = v_{\parallel} t\, \hat{k} \tag{1.3a}$$

$$\vec{r}_{\perp} = r_c\, \hat{\rho} = \frac{v_{\perp}}{\omega_c} \Big(\cos\left(\omega_c t + \phi\right) \hat{\imath} + \sin\left(\omega_c t + \phi\right) \hat{\jmath} \Big) \tag{1.3b}$$

where $v_{\parallel}$ is the velocity component parallel to the magnetic field, $r_c = \frac{v_{\perp}}{\omega_c}$ is the cyclotron radius, $\omega_c = \frac{ZeB}{m}$ is the cyclotron frequency, and ϕ is an arbitrary phase angle. A visual representation of this trajectory is shown in fig. 1.3.

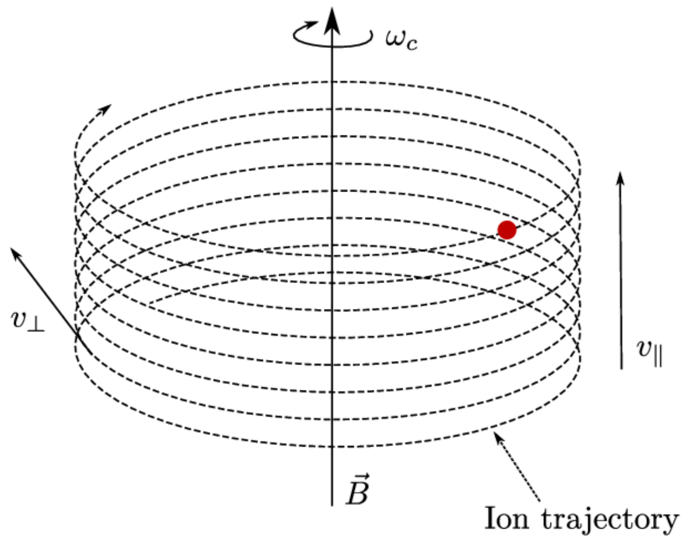

Figure 1.3: Cyclotron trajectory of an ion under the influence of a magnetic field due to the Lorentz force.

If the magnetic field lines close upon themselves, the particles become trapped in these trajectories and are thus confined within a limited region of space, preventing them from reaching the reactor walls. Currently, the two main magnetic confinement fusion devices are tokamaks, which exhibit axial symmetry (see fig. 1.4a), and stellarators, which lack axial symmetry (see fig. 1.4b).

The tokamak is a toroidal device in which the plasma is confined by a strong toroidal magnetic field B_{tor} generated by external coils surrounding the vacuum vessel. Additionally, a set of poloidal field coils located at the center of the tokamak induces a toroidal current I_p within the plasma. This current, in turn, generates a poloidal magnetic field B_{pol}, with $B_{\text{tor}} \gg B_{\text{pol}}$, ensuring radial equilibrium and preventing outward radial particle drift. The resulting total magnetic field follows a helical structure, with a strength that approximately scales as $B \propto R^{-1}$, where R is the radial distance from the torus axis.

On the other hand, the stellarator also has a toroidal topology but lacks axial symmetry. Instead, its external coils are twisted, generating a non-uniform magnetic field along the torus. Typically, stellarators exhibit a discrete symmetry. Their main advantage lies in mitigating particle drift by shaping the magnetic field lines to enhance plasma stability. Unlike tokamaks, stellarators do not require a central solenoid to induce a plasma current, thereby avoiding current-driven instabilities. This feature enables continuous operation, in contrast to tokamaks, which are constrained by their pulsed operation. However, the intricate design of stellarators makes their construction and optimization more complex. As a result, the scientific community has historically focused more on tokamaks, which remain the most advanced fusion devices. This has allowed tokamaks to reach the highest combination of temperature T, density n and confinement time τ_E.

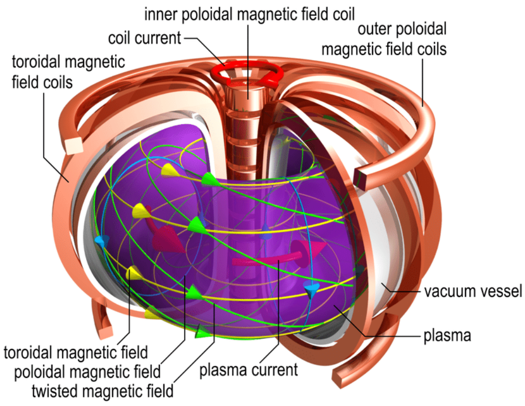

(a) Schematic of a tokamak.

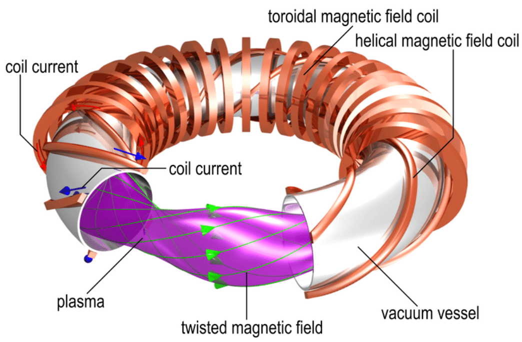

(b) Schematic of a stellarator.

Figure 1.4: Comparison between tokamak and stellarator concepts. Images adapted from [8].

The combination of these three variables (T, n, and τ_E) is known as the *triple product*, which serves as a key figure of merit in the fusion community. This is because there exists a theoretical threshold, known as the Lawson criterion eq. (1.4), beyond which a net positive energy gain is achieved from nuclear fusion reactions—that is, when the energy output exceeds the energy input required to reach sufficiently high temperatures. The energy gain is typically expressed as Q.

To date, no magnetic confinement fusion device has achieved breakeven ($Q = 1$), although ITER (*International Thermonuclear Experimental Reactor*) is expected to operate at $Q > 5$. The National Ignition Facility has reported achieving $Q > 1$ using inertial confinement fusion; however, this calculation does not account for the total energy required to power the laser beams [9].

$$nT\tau_E \geq 3.5 \times 10^{21}\,\mathrm{keV\,s\,m^{-3}} \tag{1.4}$$

1.3 Plasma heating

Regardless of the reactor type, plasma heating is a fundamental process that must be optimized to achieve $Q > 1$. One of the primary heating mechanisms is Ohmic heating, in which the kinetic energy of electrons is transferred via elastic collisions to the various plasma species. Ohmic heating is more effective in tokamaks than in stellarators due to the presence of large toroidal currents. However, its efficiency decreases at higher temperatures, as the plasma resistivity drops rapidly with increasing temperature. To overcome this limitation, alternative heating methods such as radio frequency (RF) heating and Neutral Beam Injection (NBI) are employed.

NBI involves injecting neutral particles that, being unaffected by the reactor's magnetic fields, can penetrate deeper into the plasma. Once inside, these particles undergo ionization and transfer both kinetic energy and momentum to the plasma, contributing to its heating.

Ion Cyclotron Resonance Heating (ICRH) and Electron Cyclotron Resonance Heating (ECRH) are two complementary RF heating methods used to heat the plasma. In these techniques, antennas installed along the reactor walls—illustrated in fig. 1.5—emit electromagnetic waves at frequencies that resonate with the cyclotron frequencies of either electrons or ions. This resonance facilitates efficient energy transfer from the waves to the perpendicular kinetic energy of the charged particles. Consequently, these waves propagate through the plasma, continuously interacting with its constituents and sustaining the heating process.

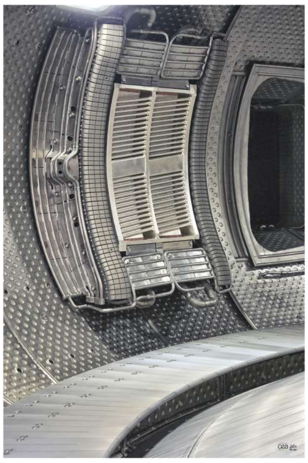

(a) ICRH in the WEST tokamak [10].

(b) ICRH in the Wendelstein 7-X stellarator [11].

Figure 1.5: Examples of ICRH antennas.

1.3.1 Ion Cyclotron Resonance Frequency Heating

In *ICRH*, the electromagnetic wave launched by the antenna is absorbed by the ions, although electrons can also absorb power. Ion absorption occurs when the ion cyclotron frequency or its harmonic matches the Doppler-shifted wave frequency:

$$\omega = k_{\parallel} v_{\parallel} + l\omega_c \qquad l \in \mathbb{N} \tag{1.5}$$

where $k_{\parallel}$ is the parallel wave number with respect to the magnetic field, and ω_c is the cyclotron frequency. The variable l represents the harmonics of the wave, where $l = 1$ is the fundamental wave and $l > 1$ are the higher harmonics. Since the cyclotron frequency is proportional to $\omega_c \propto B \propto R^{-1}$, the location of the absorption can be controlled, allowing for precise heating of a specific area inside the reactor.

The electric field of an electromagnetic wave can be divided into two components: one parallel to the background magnetic field and one perpendicular. The parallel component is small for waves in the ion cyclotron range of frequencies and can be neglected, while the perpendicular component can be further divided into two components: a left circularly polarized component (E_+) and a right circularly polarized component (E_-). E_+ rotates in the same direction as the ions, while E_- counter-rotates. If the angle between E_+ and the perpendicular velocity of the ion remains constant, it will give rise to a net acceleration. This process increases the energy of the ions and modifies the tail (high-energy part) of the distribution function.

For fundamental harmonic heating, neglecting the perpendicular wave number ($k_\perp \sim 0$) and assuming $v_\perp = v_x + iv_y$, the differential equation for the evolution of the velocity yields:

$$v_\perp = v_0 e^{-i\omega_c t} + \frac{eE_+}{m} t e^{-i\omega_c t} \tag{1.6}$$

Here, v_0 is the initial velocity and m is the ion mass. The first and second terms are always in phase, thus resulting in a net acceleration.

The physics of absorption at higher harmonics is more complicated. For example, for the second harmonic, the resonance between the particle and the wave is lost. However, if the wave changes its amplitude in space, the particles will no longer be driven by a spatially uniform sine wave in time. This can lead to a resonance condition, which occurs when the wavelength and the Larmor radius (the radius of the ion's orbit around the magnetic field) are comparable. As a result, the perpendicular wave number is no longer negligible ($k_\perp \neq 0$). This phenomenon is known as the finite Larmor radius effect (FLR) and is responsible for absorption at higher harmonics.

2
Objectives

The scope of this thesis falls within a larger project led by the Fusion Group at the BSC, named **Alya4fusion**. Alya [12] is a development framework that enables the modeling of different physical phenomena using the Finite Element Method (FEM). This software provides parallelism tools in an integrated and transparent manner to the developer. Alya4fusion will consist of a series of independent yet coupled modules capable of solving numerous complex physics problems commonly encountered in nuclear fusion reactors—problems that are generally difficult to predict analytically. This framework will enable the simultaneous execution of multiple simulations, collectively functioning as a Digital Twin of a nuclear fusion reactor. Some examples of developed, tested, and benchmarked modules within Alya4fusion include NEUTRO [13, 14] and MAGNET [15].

This PhD thesis research will focus on magnetically confined nuclear fusion and plasma physics engineering, independent of reactor geometry and design, and will integrate state-of-the-art techniques from fields such as numerical simulations, high-performance computing (HPC), parallel computing, artificial intelligence (AI), and machine learning (ML). Ultimately, the goal of this thesis is to develop **EMWAVE**, a software module capable of running in HPC environments to simulate the ICRH and ECRH mechanisms within a nuclear fusion reactor.

2.1 Modelling Present-Day and Future ICRH Scenarios

The primary objective of this PhD thesis is to develop a tool capable of simulating ICRH and ECRH, which will require most of the time and dedication of this project. Simulating wave propagation, particle-wave interactions, particle transport, and resonances demands a highly precise solver capable of modelling a hot plasma medium in a fully 3D reactor geometry.

Currently, the state of the code under development allows for the simulation of wave propagation in a 2D cross-section of a cold plasma domain. Therefore, some of the main subtasks will be:

- Extending the current module and its solver to simulate the full wave equation in a 3D reactor domain.
- Implementing a fully populated permittivity tensor to account for a hot plasma medium, in contrast to cold plasma, which behaves as a gyroelectric material.
- Completing the migration to the HPC environment Alya and parallelising the code accordingly to optimize resource usage.

Once these issues are addressed, the code will be capable of simulating many relevant present-day scenarios and will contribute to the design and optimization of future fusion reactors.

2.2 Hot Plasma Tensor Calculation

Migrating to a more general permittivity tensor not only fundamentally alters the equation to be solved but also introduces the challenge of accurately computing the tensor's internal parameters. This theoretical framework incorporates the velocity distribution of particles and their binary collisions. Typically, the distribution function is assumed to follow a Maxwellian form, simplifying the calculation of the permittivity tensor, or a Fokker-Planck distribution, which is extremely computationally demanding. However, achieving a more precise description of the phenomena and obtaining higher accuracy in the results would require a dedicated module for computing the particle energy distribution.

2.3 Implementing AI and ML

Once the code is functioning correctly and meets the required criteria for accuracy, an important step will be to incorporate data-driven or physics-informed algorithms to:

- Speed up the solving process, for example, by providing an initial solution or preconditioning.
- Optimize operational parameters, enabling better adaptive control.
- Implement AI-driven meshing techniques and adaptive refinement to reduce computational costs.
- Identify propagation patterns or instabilities by analyzing large datasets with ML models.

Beyond improving the simulation capabilities for ICRH and ECRH scenarios, integrating AI and ML into this research can provide valuable insights that contribute to advancements in both artificial intelligence and computational plasma physics. The development of novel AI-driven techniques for wave modeling, optimization, and data analysis could also benefit broader areas of plasma physics and nuclear fusion engineering, paving the way for more efficient reactor designs and predictive control strategies.

3
State of the Art in Modelling ICRH

Before discussing the state of the art in computational plasma physics, it is important to clarify that this project originated as part of the author's Master's Thesis [16]. The initial stages were conducted during the Master's program, focusing on the development of a Fortran code from scratch. The objective was to simulate both a plane wave and a finite-source wave propagating through conventional dielectric, gyroelectric media, and inhomogeneous cold plasma. This early work laid the foundation for future implementation within Alya. The standalone code serves as a benchmark sandbox, enabling testing and development without major repercussions for other developers or environments.

The primary role of ICRH is to heat ions in the plasma using the fast magnetosonic wave (here referred to as the fast wave). Other important applications include the heating of electrons, non-inductive current drive, the generation of fast ions, wall conditioning, sawtooth stabilization, and the control of impurities and rotational profiles.

Several codes have been developed to simulate RF heating, each with specific limitations and applications. These codes are based on FEM, Fourier spectral methods, finite differences or a combination of both [17–21]. Most ICRH modelling tools either focus on a detailed representation of the plasma but use a simplified representation of the SOL and antennas. Conversely, dedicated antenna codes employ a more accurate description of antennas, enabling detailed studies of, e.g., coupling and antenna spectra, but rely on more simplified plasma core models [22].

In [23], a modeling technique that accurately represents both the core plasma and the SOL and antenna region is described. This is achieved by using an FEM-based code for regions outside the separatrix, while the core plasma is described using the TORIC code [24]. A mode-matching technique is used to couple these two codes.

On the other hand, EVE, a variational method-based code [21], does not allow for self-consistent modeling of antenna-plasma coupling [25].

ERMES [26, 27], which has been used for benchmarking our code, is restricted to cold plasma media and applies only in the vicinity of antennas. Other notable codes within the fusion community include TORIC [24], TOPICA [22], SCENIC [28], PION [29], AORSA [30], and the model proposed in [31].

Efforts have been made within the Fusion Group to adapt and install AORSA on MareNostrum4. However, since it operates independently of Alya and other codes, it cannot be integrated into an engineering-coupled framework. Similarly, PION has been extensively used within the Fusion Group to model certain aspects of ICRF in JET (*Joint European Torus*), AUG (*ASDEX Upgrade*) and ITER [32, 33].

Another example is COMSOL, a commercial software that employs the finite element method (FEM) and supports multiphysics coupling, although it is not specifically designed for HPC environments. Despite not being dedicated to plasma physics, various COMSOL modules have been developed to simulate electromagnetic fields in a cold plasma near antennas [34] or in the scrape-off layer for lower-hybrid heating mode [35].

Each of these codes presents specific constraints: they may be limited to certain plasma regions, rely on simplified models for the plasma or antenna, require coupling between different codes, or lack built-in support for high-performance computing. EMWAVE aims to be the first code embedded within an HPC framework capable of simulating the entire reactor-shaped domain. Its design enables integration with a network of other modules, working together to model the various physical phenomena in a nuclear fusion reactor. The resulting digital twin of the reactor will play a key role in the design and optimization of both current and future fusion devices.

To date, no European research group is known to be actively pursuing this approach. However, the Oak Ridge National Laboratory in the United States has a research team working on a similar goal [36].

4 Methodology

Although different objectives are proposed for this thesis, the main and key task will be the development of numerical software for wave propagation simulation. Therefore, the methodology of this work will focus primarily on achieving this goal. The implementation of AI and ML will be carried out under the guidance of experts in the field and with the knowledge acquired by the author throughout the Ph.D. program. Additionally, this task will most likely take place in the final stages of the Ph.D. On the other hand, new challenges and objectives that may arise during the research will be addressed using the best approach possible at the time.

4.1 Alya

This Ph.D. thesis will primarily contribute to the development of FEM software in Alya [12] to simulate ICRH and ECRH in plasma fusion. Alya is more than just a Finite Element Method (FEM) code; it is a development framework where different physics are implemented according to the developer's interests. Alya provides parallelism tools in an integrated and transparent manner to the developer and was designed from the very first line of code to achieve the best possible performance on a supercomputer. As a result, efficiencies close to 100% are obtained even when running problems on 100,000 processors [12].

Alya's kernel includes a mesh partitioning system, I/O management, a large number of linear system and eigenvalue solvers, and an extensive finite element library, which serves as its main numerical tool. Various specific modules are built on this kernel to solve problems of interest. Currently, there are modules for solving thermal problems, incompressible fluid dynamics, turbulence, structural mechanics, combustion, neutronics, and magnetism, among others. The Fusion Group is responsible for developing and maintaining several modules, such as NEUTRO, which describes neutron transport [13, 14], MAGNET, which models magnetic behavior in superconductors [15], and EQUILI, a new module that generates equilibrium in a plasma domain [37].

With these developments, Alya will incorporate the necessary plasma physics capabilities, all within a unified framework that shares the same language, I/O system, and numerical technology while benefiting from the natural communication provided by the kernel. Additionally, this software will take advantage of Alya's high computational efficiency and continuous support for optimizing the kernel across different architectures.

4.2 Finite Element Method

The Finite Element Method (FEM) is a well-established numerical tool that allows solving linear and nonlinear partial differential equations (PDEs) in a physical domain, constrained by a set of boundary conditions. These kinds of problems are known as *boundary value problems* (BVPs). The algorithm is not limited to a particular domain shape, size, or set of PDEs, making it highly adaptable and applicable to various fields of physics. The Finite Element Method was first used in the 1940s by Alexander Hrennikoff and Richard Courant and was initially applied to the calculation of mechanical stress and elastic deformations in continuous solids [38, 39].

The main principle of FEM is the division of a computational domain into a set of *finite elements*, forming a mesh structure where the differential equation will be solved. Each element has a series of nodes or coordinate points, depending on the element's shape and the order of approximation. For example, the most common elements used are triangles and quadrilaterals for 2D meshes or tetrahedra and hexahedra for 3D meshes. Within an element, the unknown function to be determined is represented as a linear combination of a series of basis functions. These basis functions, commonly known as *shape functions*, can be linear, quadratic, or even higher-order polynomials. Within each element, a local system of algebraic equations is constructed, and by leveraging the connectivity between elements, a global set of linear equations is assembled. The number of nodes in a given element depends only on the polynomial order of the shape functions; for instance, an element can be linear or quadratic with a triangular or quadrilateral shape. Higher-order elements also exist, such as cubic elements or a specific case of the quadrilateral quadratic element known as the Lagrangian element.

When transitioning to a 3D domain and solving a vectorial wave equation, a new approach within FEM will be required. Conventional nodal-based elements (elements whose solution is computed at the nodes) present several challenges when dealing with vector fields, such as spurious solutions, field singularities, and difficulties in imposing boundary conditions on material interfaces [40]. Some of these problems arise from the fact that nodal elements do not enforce the divergence condition (i.e., the divergence of the field is zero). Fortunately, in the 1980s, edge elements began to be applied, introducing significant improvements in the field. In short, edge elements use a vector basis that assigns degrees of freedom to the edges of the elements rather than to the nodes. The implementation of these elements will be crucial for the future development of EMWAVE.

4.3 Cold and Hot Plasma Models

4.3.1 Cold Plasma

The current implementation of EMWAVE does not take into account the thermal distribution of particles or the effects of heating methods such as the ICRH. Instead, the plasma is treated under the cold plasma approximation, which assumes that the thermal velocity of particles is much smaller than the phase velocity of an injected wave. This approximation is necessary due to the early stage of EMWAVE development, where a time-harmonic equation is solved, requiring a time-independent permittivity tensor.

Despite its limitations, the cold plasma model provides a reasonable estimation of the wave's ability to reach the plasma region of interest. The code evaluates whether an electromagnetic wave can propagate in an arbitrary linear medium, such as plasma. Although wave-particle interactions are neglected, the model remains useful for assessing wave accessibility.

Within this framework, the permittivity tensor, which plays a fundamental role in the partial differential equation to be solved, is expressed as

$$\varepsilon_r = \begin{pmatrix} \varepsilon_\perp & -i\varepsilon_{xy} & 0 \\ i\varepsilon_{xy} & \varepsilon_\perp & 0 \\ 0 & 0 & \varepsilon_\parallel \end{pmatrix} = \begin{pmatrix} S & -iD & 0 \\ iD & S & 0 \\ 0 & 0 & P \end{pmatrix} \tag{4.1}$$

with the components

$$\varepsilon_\perp = S = \frac{R+L}{2} = 1 - \sum_j \frac{\omega_{pj}^2}{\omega^2 - \omega_{cj}^2} \tag{4.2a}$$

$$\varepsilon_{xy} = D = \frac{R-L}{2} = \sum_j \frac{\omega_{cj}\omega_{pj}^2}{\omega\left(\omega^2 - \omega_{cj}^2\right)} \tag{4.2b}$$

$$\varepsilon_\parallel = P = 1 - \sum_j \frac{\omega_{pj}^2}{\omega^2} \tag{4.2c}$$

$$R = S + D = 1 - \sum_j \frac{\omega_{pj}^2}{\omega\left(\omega + \omega_{cj}\right)} \tag{4.2d}$$

$$L = S - D = 1 - \sum_j \frac{\omega_{pj}^2}{\omega\left(\omega - \omega_{cj}\right)} \tag{4.2e}$$

where the cyclotron and plasma frequencies are defined as

$$\omega_c = \frac{qB_0}{m}, \quad \omega_{pj}^2 = \frac{n_j\left(Z_j e\right)^2}{\varepsilon_0 m_j}. \tag{4.3}$$

The cold plasma permittivity tensor eq. (4.1) corresponds to a gyroelectric material tensor. The presence of zero values in ε_{xz}, ε_{zx}, ε_{yz}, and ε_{zy}, together with the assumption of z-invariance ($\partial_z = 0$), enables the decomposition of the wave into two independent polarisations in a 2D cross-section geometry.

4.3.2 Hot Plasma

The hot plasma model considers cases where the thermal velocity of ions is comparable to or greater than the phase velocity of the electromagnetic wave. To describe this scenario, kinetic theory must be introduced. This theoretical framework incorporates the velocity distribution of particles and the binary collisions between them.

By assuming a specific distribution function—typically Maxwellian or Fokker-Planck distributions— it is possible to derive the permittivity tensor for a hot plasma medium. However, the mathematical procedure becomes significantly more complex, making a full derivation beyond the scope of this manuscript. Nevertheless, a general expression for the permittivity tensor can be written as

$$\varepsilon_r = \begin{pmatrix} K_1 + \sin^2(\psi)K_0 & K_2 - \cos(\psi)\sin(\psi)K_0 & \cos(\psi)K_4 + \sin(\psi)K_5 \\ -K_2 - \cos(\psi)\sin(\psi)K_0 & K_1 + \cos^2(\psi)K_0 & \sin(\psi)K_4 - \cos(\psi)K_5 \\ \cos(\psi)K_4 - \sin(\psi)K_5 & \sin(\psi)K_4 + \cos(\psi)K_5 & K_3 \end{pmatrix} \tag{4.4}$$

where ψ represents the angle between k_x and k_y, and $\{K_i\}_{i=1}^{6}$ is a set of parameters with lengthy and complex expressions. These parameters depend on multiple factors, including modified Bessel functions, plasma dispersion functions, frequencies, temperatures, wave vectors, and other physical quantities.

In this model, the wave equations become more intricate, making it impossible to decouple specific polarizations. Due to the general structure of the permittivity tensor, each field component is inherently dependent on the others.

5
Programme Schedule

When undertaking an ambitious project such as a Ph.D., careful planning and the establishment of milestones are essential to maintaining focus on long-term objectives. However, the inherently unpredictable nature of research means that plans are always subject to modification. For this reason, the schedule presented here serves as an indicative guide rather than a strictly rigid timeline.

This Ph.D. thesis is funded for a duration of four years, which defines the overall timeframe for its development.

5.1 Timeline

This section provides an overview of the thesis timeline through an indicative Gantt chart (fig. 5.1).

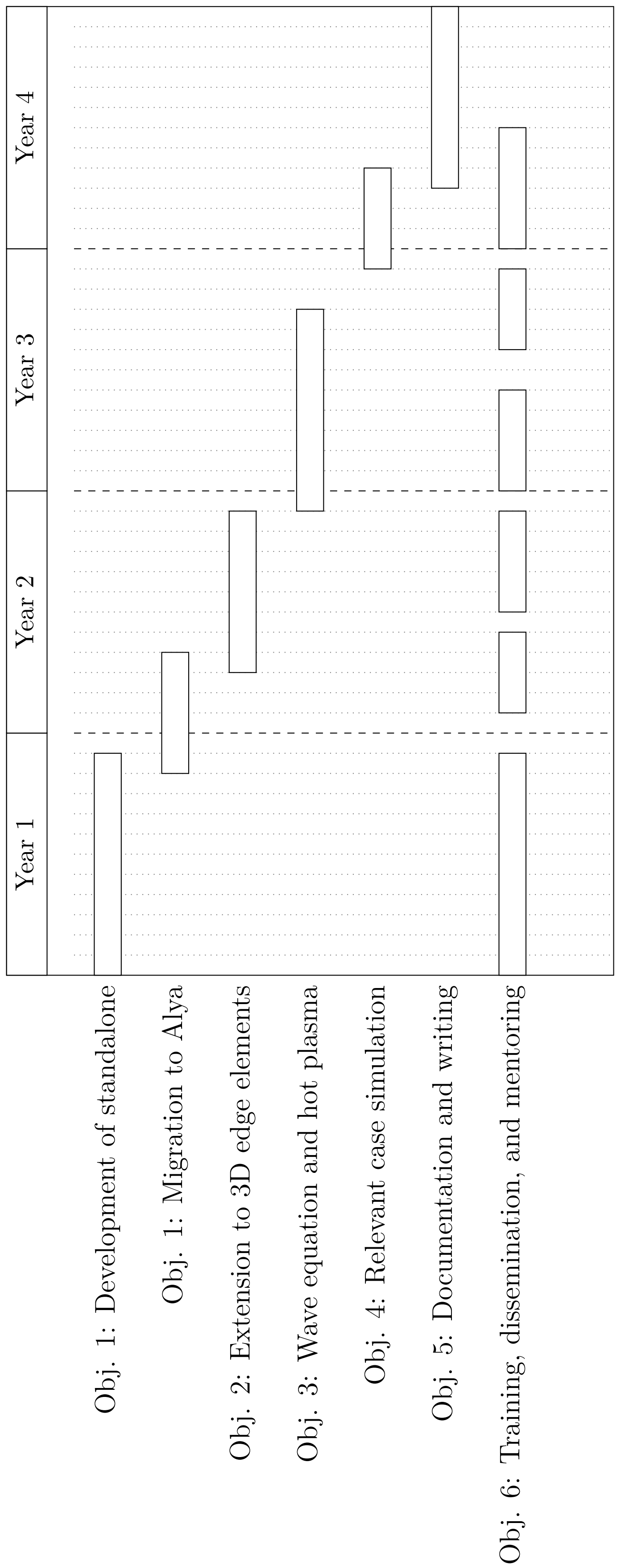

Figure 5.1: Gantt Diagram for PhD's project.

Appendices

A
Previous Achievements

As mentioned in chapter 3, this project was initiated during the Master's Thesis [16], where the foundations of the work were established by simulating a plane wave propagating and dispersing in conventional dielectrics, anisotropic dielectrics, gyroelectric media, and inhomogeneous cold plasma. The code was initially executed on a conventional PC, awaiting migration to Alya during the first year of the Ph.D.

Nonetheless, interesting results have been achieved so far. For example, we have been able to reproduce plane wave dispersion in conventional and anisotropic dielectrics, as well as in homogeneous and inhomogeneous magnetized cold plasma, for different domain truncation methods: either Perfectly Matched Layers (PML) or Absorbing Boundary Conditions (ABC). Furthermore, these cases have been developed and tested in both the standalone version of the code and the Alya framework. Additionally, simplified versions of the antenna have been implemented in the standalone version and are currently being migrated to Alya.

For example, in fig. A.1a, the field distribution for a fast wave propagating through an isotropic homogeneous dielectric can be observed, whereas in fig. A.1b, the permittivity presents anisotropy. Both simulations employed PML as a truncation layer.

In fig. A.2a, the same case as in fig. A.1a is shown but with an ABC, which is more efficient when using parallel computing. In fig. A.2b, a particular case of

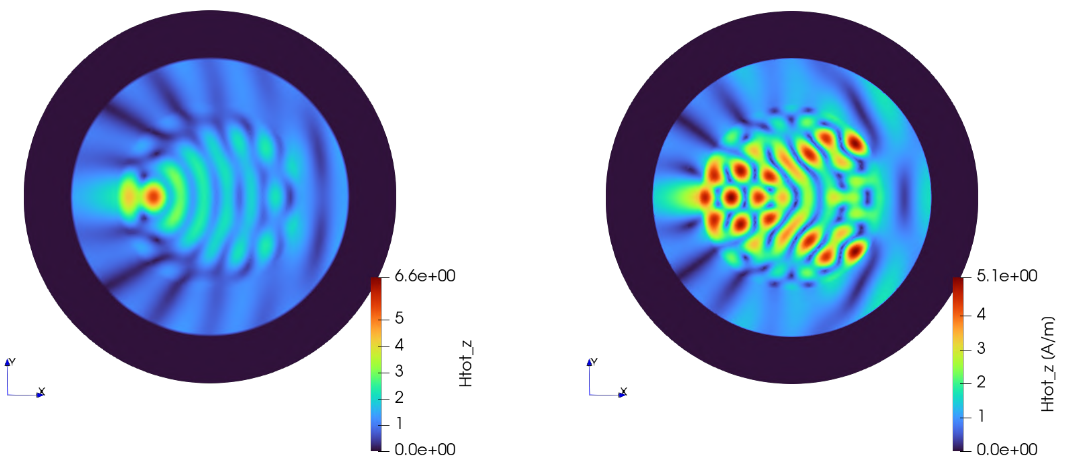

(a) $\varepsilon_{xx} = \varepsilon_{yy} = 4$. **(b)** $\varepsilon_{xx} = 9$, $\varepsilon_{yy} = 4$.

Figure A.1: H_z^{tot} amplitude distribution for a fast wave, with PML as the truncation method.

a homogeneous gyroelectric material is presented. This case was benchmarked successfully against [27].

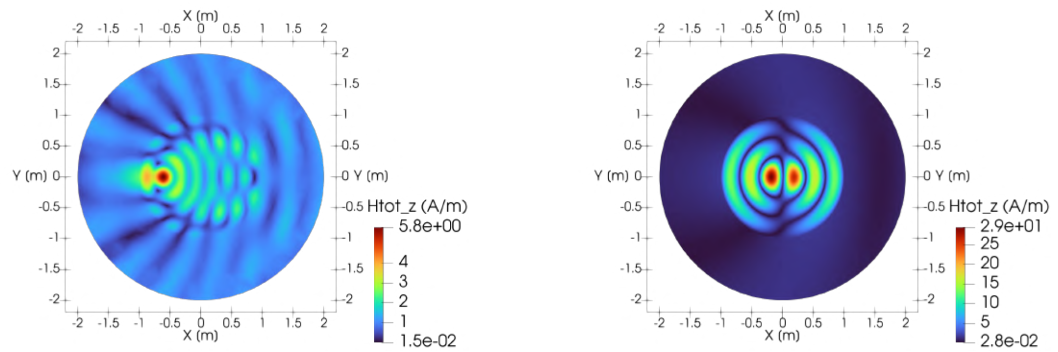

(a) $\varepsilon_{xx} = \varepsilon_{yy} = 4$. **(b)** Homogeneous cold plasma.

Figure A.2: H_z^{tot} amplitude distribution for a fast wave, with ABC as the truncation method.

One important aspect that was verified during the development of the code was whether it correctly accounted for cutoff regions, where the wave can no longer propagate through the plasma. This occurs when the refractive index satisfies $n^2 \lesssim 0$. This verification is crucial for assessing wave accessibility. It is relevant to note that these simulations were performed with a homogeneous permittivity tensor. In fig. A.3, an ordinary wave (also known as a slow wave) is shown, with a frequency smaller than the plasma frequency. Similarly, fig. A.4a ($L = 0$) and fig. A.4b ($R = 0$) illustrate cases where the refractive index becomes zero for the fast wave, preventing its propagation.

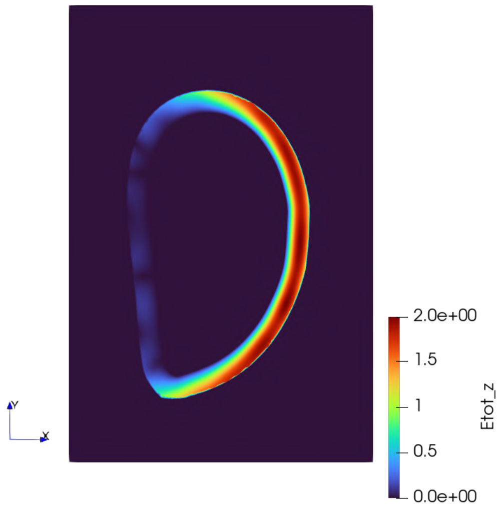

Figure A.3: $E_z^{\rm tot}$ field for an ordinary wave with $\omega < \omega_p$ cutoff.

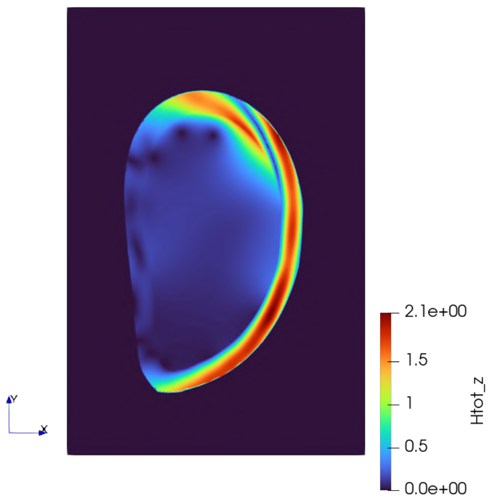

(a) $H_z^{\rm tot}$ field at L-cutoff.

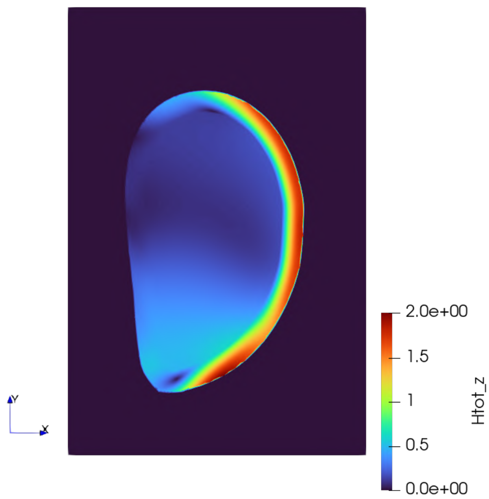

(b) $H_z^{\rm tot}$ field at R-cutoff.

Figure A.4: The extraordinary wave is unable to propagate when $n_X \approx 0$.

Finally, another significant result was obtained when testing the second tritium scenario, one of the main ICRF heating scenarios in ITER [41]. It was observed that the fast wave exhibits excellent accessibility throughout the entire plasma domain, as expected. In fig. A.5a, the field amplitude can be observed when radiation originates from an antenna with an associated arbitrary current density. On the other hand, fig. A.5b presents the same case but with a plane wave instead.

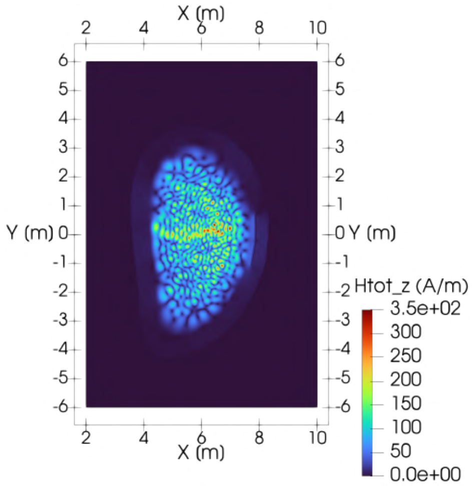

(a) Radiation from an antenna source with PML.

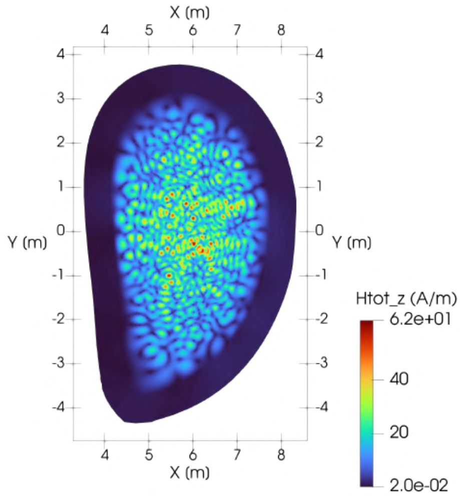

(b) Plane wave radiation with ABC.

Figure A.5: H_z^{tot} amplitude for the second tritium harmonic scenario.

In parallel, since the beginning of the Master's Thesis, several activities and notable events have taken place, including:

- Participation in the 11th BSC International Symposium, presenting the work carried out in the early months of the Master's Thesis.
- Participation in the 5th Fusion HPC Workshop, showcasing the progress made by the end of the Master's Thesis to an international audience.
- Mentoring students during their internships at the Fusion Group in BSC.
- Writing several abstracts, currently under review, for participation in leading research conferences, such as the 51st EPS Conference on Plasma Physics and the 51st Annual Plasma Physics Conference.

B
Data Management Plan

In this appendix, the Data Management Plan (DMP) for this thesis is presented. Data management will not play a key role during the thesis, as no critical or confidential data will be collected at any point. However, it will be an important aspect to consider when simulating a large number of scenarios on the HPC cluster, as this will generate a significant amount of data. This aspect will need to be carefully managed, but it is not a primary focus at the moment.

Plan Overview

A Data Management Plan created using CORA.eiNa DMP

Title: EMWAVE: A FEM code to simulate wave propagation in magnetically confined plasma domains

Creator: Hernán Domingo Ramos
Affiliation: Universitat Politècnica de Catalunya

Template: Doctorand UPC (English)

DMP ID: 6375

Last modified: 21-02-2025

Project abstract:

The pursuit of sustainable and efficient energy sources has placed nuclear fusion at the forefront of scientific research. This Ph.D. project focuses on developing **EMWAVE**, a high-performance **finite element method (FEM)** code to simulate **wave propagation in magnetically confined plasmas**, specifically targeting **Ion Cyclotron Resonance Heating (ICRH) and Electron Cyclotron Resonance Heating (ECRH)** in fusion reactors. The work is part of the **Alya4fusion** initiative at the **Barcelona Supercomputing Center (BSC)**, aiming to create a digital twin of fusion reactors by integrating various computational models.

The research has three primary objectives: (1) Extending the current **cold plasma** wave propagation solver to **fully three-dimensional** reactor domains, incorporating a **hot plasma tensor** to capture kinetic effects; (2) Enhancing accuracy by improving the **permittivity tensor computation**, which considers the velocity distribution of particles; and (3) Implementing **artificial intelligence (AI) and machine learning (ML)** techniques to optimize simulations, accelerate computations, and refine meshing strategies.

The methodology relies on the **Alya HPC framework**, leveraging **edge elements** to mitigate numerical artifacts in electromagnetic simulations. EMWAVE aims to surpass existing codes, such as **ERMES, TORIC, and AORSA**, by integrating with an HPC ecosystem for large-scale fusion reactor modeling. The research will contribute to designing next-generation fusion devices and optimizing heating schemes, pushing toward a more viable and efficient realization of nuclear fusion energy.

Start date: 19-08-2024

End date: 20-08-2028

EMWAVE: A FEM code to simulate wave propagation in magnetically confined plasma domains

About your research

Hernán Domingo Ramos
hernan.domingo@upc.edu

Shimpei Futatani
shimpei.futatani@upc.edu

EMWAVE: A FEM code to simulate wave propagation in magnetically confined plasma domains

My research is focused on the development of a software tool within Alya, an HPC framework developed by the CASE group in the BSC. EMWAVE will simulate ICRF and ECRF in magnetically confined plasma fusion reactors using the finite element method (FEM), using 3D domains and hot plasma models. This PhD will also explore the integration of AI and ML to accelerate simulations and extract extra insight from simulation results.

Start date: 19-08-2024
End date: 20-09-2028

This thesis is related to the Alya4fusion project. Alya4fusion aims to simulate a number of relevant multi-physics processes in a fusion reactor by leveraging high-performance computing (HPC) and artificial intelligence (AI) through MareNostrum 5, a pre-exascale European-funded supercomputer at BSC. Alya4fusion comprises several independent yet coupled code modules. The Fusion Group has already developed NEUTRO and MAGNET, while two more are underway: EQUILI, which computes plasma equilibrium, and EMWAVE, which simulates electromagnetic wave propagation and absorption in plasma environments.

The funding of my PhD program comes from the Barcelona Supercomputing Center Fellowships AI4S.

About this data management plan

20-02-2025

21-02-2025

v1
21-02-2025

1. Data Collection

- Your own data or data from the research group in which you participate
- Academic collaborators

I will generate my own data.
If needed for benchmarking I will ask for permission and reuse academic collaborators' data.

You can use a table similar to the one below (which contains examples) to describe the type of data in your research

Data type	Format	Reuse of existing data	Data origin	Estimated size	Data utility (how will be reused?)
Observational	(.doc); (.pdf)	Yes. Journal publications	Scientific Journals	30-50 GB	For code benchmarking and testing
Spreadsheets	(.csv); (.dat)	No	Research	>2TB	

- I'm not working with personal or sensitive data

2. Documentation and data quality

I will differentiate between mesh folders and results folders.
Mesh files and folders will have the naming TS-XXXXXX\TS-XXXXXXX.YYY.dat
where TS stands for Test Suite, XXXXX is the case's name, and YYY is the type of input file.
Results files will be named Results\TS-XXXXXXX\TS-XXXXXXX_POL_ZZZ.ensi.case
Where XXXX is the case's name again, POL will be the type of polarisation, and ZZZ will be an alphanumeric identification for the permittivity type of the problem. *ensi.case* is the format that the code generates.

- Version number and date in the file or folder name

The code is tracked with Git, ensuring version control. Results' versions will be tracked only by their name.

- Readme files

The input files will be almost self-explanatory, but extra files will be added to ensure robust information.

There is no planned metadata repository apart from readme files.

3. Data storage and security during your research

- Access restrictions
- Regular backups

There is no commercial and ethical restriction, only subjected to common confidentiality in scientific research. Data will be stored in several hard copies safeguarded by pa

There are no major security risks, apart from the inconvenience of re-executing the code or re-meshing the domains. Hopefully, it could be recovered with well-planned backups.

- Physical storage (e.g., USB, external hard drive)
- In the network of your department or research group

The files will be partially stored on physical devices but also in the data infrastructure of the BSC.

4. Legal and ethical requiriments

- No

- No

- Managed access procedure in place for authorised users of personal data
- Gain informed consent for preservation and/or sharing of personal data
- Anonymisation of personal data for preservation and/or sharing
- Pseudonymisation of personal data
- Encryption of personal data

N/A

I will be the owner of the data that my software produces.
The data will not be openly accessible until it is published.

There is no ethical issues.

5. Access, share and reuse the data

No restrictions.

My data will be available to the public through scientific publications and conferences.

CC-BY-NC

6. Deposit and conservation of the data

- Type of data (raw, processed) and ease of generation
- Relevance of content to others
- Data linked to a publication

10 years

- UPC data instutional repository (e.g., CORA. Repositori de Dades de Recerca)

References

[1] Dario Maradin. “Advantages and Disadvantages of Renewable Energy Sources Utilization”. en. In: *International Journal of Energy Economics and Policy* 11.3 (Apr. 2021). Number: 3, pp. 176–183. URL: `https://econjournals.com/index.php/ijeep/article/view/11027` (visited on 02/20/2025).

[2] Francisco Júnior Freires et al. “Advantages and disadvantages of renewable energy: a review of the scientific literature”. en. In: *Revista de Gestão e Secretariado* 14.11 (Nov. 2023), pp. 20221–20240. URL: `https://ojs.revistagesec.org.br/secretariado/article/view/3174` (visited on 02/20/2025).

[3] Jeffrey P. Freidberg. *Plasma Physics and Fusion Energy*. Cambridge: Cambridge University Press, 2007. URL: `https://www.cambridge.org/core/books/plasma-physics-and-fusion-energy/CD7B530D2889F70446F34E14EE0EF703` (visited on 05/23/2024).

[4] Francis F. Chen. *Introduction to Plasma Physics and Controlled Fusion*. en. Cham: Springer International Publishing, 2016. URL: `http://link.springer.com/10.1007/978-3-319-22309-4` (visited on 02/20/2025).

[5] M. B. Chadwick et al. “ENDF/B-VII.1 Nuclear Data for Science and Technology: Cross Sections, Covariances, Fission Product Yields and Decay Data”. In: *Nuclear Data Sheets*. Special Issue on ENDF/B-VII.1 Library 112.12 (Dec. 2011), pp. 2887–2996. URL: `https://www.sciencedirect.com/science/article/pii/S009037521100113X` (visited on 02/20/2025).

[6] D. A. Brown et al. “ENDF/B-VIII.0: The 8th Major Release of the Nuclear Reaction Data Library with CIELO-project Cross Sections, New Standards and Thermal Scattering Data”. In: *Nuclear Data Sheets*. Special Issue on Nuclear Reaction Data 148 (Feb. 2018), pp. 1–142. URL: `https://www.sciencedirect.com/science/article/pii/S0090375218300206` (visited on 02/20/2025).

[7] Susanne Pfalzner. *An Introduction to Inertial Confinement Fusion*. Boca Raton: CRC Press, Mar. 2006.

[8] Josefine Henriette Elise Proll. “Trapped-particle instabilities in quasi-isodynamic stellarators”. en. PhD thesis. Institut für Physik, 2014.

[9] David Kramer. “National Ignition Facility surpasses long-awaited fusion milestone”. English. In: *Physics Today* (Dec. 2022). URL: `https://pubs.aip.org/physicstoday/online/41898/National-Ignition-Facility-surpasses-long-awaited` (visited on 02/14/2025).

[10] J. Hillairet et al. “WEST actively cooled load resilient ion cyclotron resonance heating system results”. en. In: *Nuclear Fusion* 61.9 (Aug. 2021). Publisher: IOP Publishing, p. 096030. URL: `https://dx.doi.org/10.1088/1741-4326/ac1759` (visited on 02/20/2025).

[11] Max-Planck-Gesellschaft. *ICRH*. en. URL: `https://www.ipp.mpg.de/3871973/ICRH` (visited on 02/20/2025).

[12] Mariano Vázquez et al. “Alya: Multiphysics engineering simulation toward exascale”. In: *Journal of Computational Science*. The Route to Exascale: Novel Mathematical Methods, Scalable Algorithms and Computational Science Skills 14 (May 2016), pp. 15–27. URL: `https://www.sciencedirect.com/science/article/pii/S1877750315300521` (visited on 02/20/2025).

[13] Albert Gutierrez-Milla et al. “New high performance computing software for multiphysics simulations of fusion reactors”. In: *Fusion Engineering and Design*. Special Issue: Proceedings of the 13th International Symposium on Fusion Nuclear Technology (ISFNT-13) 136 (Nov. 2018), pp. 639–644. URL: `https://www.sciencedirect.com/science/article/pii/S0920379618302643` (visited on 02/20/2025).

[14] E Goldberg et al. “Validating NEUTRO, a deterministic finite element neutron transport solver for fusion applications, with literature tests, experimental benchmarks and other neutronic codes”. en. In: *Plasma Physics and Controlled Fusion* 64.10 (Aug. 2022). Publisher: IOP Publishing, p. 104006. URL: `https://dx.doi.org/10.1088/1361-6587/ac8acd` (visited on 02/20/2025).

[15] A. Soba et al. “A high-performance electromagnetic code to simulate high-temperature superconductors”. In: *Fusion Engineering and Design* 201 (Apr. 2024), p. 114282. URL: `https://www.sciencedirect.com/science/article/pii/S0920379624001352` (visited on 02/20/2025).

[16] Hernán Domingo Ramos. “MAXWEL: FEM software module to compute EM fields within a magnetically confined fusion reactor”. English. MA thesis. Ghent: Ghent University, Aug. 2024. URL: `http://fusion.bsc.es/wp-content/uploads/Hernan_Domingo_Ramos_MSc_Thesis_manuscript_compressed.pdf`.

[17] Pavel Popovich, W. Anthony Cooper, and Laurent Villard. “Three-Dimensional Full-Wave Propagation Code for Cold Plasma”. In: *Fusion Science and Technology* 46.2 (Sept. 2004). Publisher: American Nuclear Society _eprint: https://doi.org/10.13182/FST04-A573, pp. 342–347. URL: `https://doi.org/10.13182/FST04-A573` (visited on 02/21/2025).

[18] M. Brambilla and R. Bilato. “Simulation of ion cyclotron heating of tokamak plasmas using coupled Maxwell and quasilinear-Fokker–Planck solvers”. en. In: *Nuclear Fusion* 46.7 (June 2006), S387. URL: `https://dx.doi.org/10.1088/0029-5515/46/7/S01` (visited on 02/21/2025).

[19] E. F. Jaeger et al. “Advances in full-wave modeling of radio frequency heated, multidimensional plasmas”. In: *Physics of Plasmas* 9.5 (May 2002), pp. 1873–1881. URL: `https://doi.org/10.1063/1.1455001` (visited on 02/21/2025).

[20] L. Villard, S. Brunner, and J. Vaclavik. "Global marginal stability of TAEs in the presence of fast ions". en. In: *Nuclear Fusion* 35.10 (Oct. 1995), p. 1173. URL: https://dx.doi.org/10.1088/0029-5515/35/10/I03 (visited on 02/21/2025).

[21] R.J. Dumont. "Variational approach to radiofrequency waves in magnetic fusion devices". en. In: *Nuclear Fusion* 49.7 (July 2009), p. 075033. URL: https://dx.doi.org/10.1088/0029-5515/49/7/075033 (visited on 02/20/2025).

[22] V. Lancellotti et al. "TOPICA: an accurate and efficient numerical tool for analysis and design of ICRF antennas". en. In: *Nuclear Fusion* 46.7 (June 2006), S476. URL: https://dx.doi.org/10.1088/0029-5515/46/7/S10 (visited on 02/20/2025).

[23] J. Wright and S. Shiraiwa. "Antenna to Core: A New Approach to RF Modelling". en. In: *EPJ Web of Conferences* 157 (2017). Publisher: EDP Sciences, p. 02011. URL: https://www.epj-conferences.org/articles/epjconf/abs/2017/26/epjconf_rfppc2017_02011/epjconf_rfppc2017_02011.html (visited on 02/21/2025).

[24] M. Brambilla. "Numerical simulation of ion cyclotron waves in tokamak plasmas". en. In: *Plasma Physics and Controlled Fusion* 41.1 (Jan. 1999), p. 1. URL: https://dx.doi.org/10.1088/0741-3335/41/1/002 (visited on 02/20/2025).

[25] R.J. Dumont and D. Zarzoso. "Heating and current drive by ion cyclotron waves in the activated phase of ITER". en. In: *Nuclear Fusion* 53.1 (Dec. 2012). Publisher: IOP Publishing and International Atomic Energy Agency, p. 013002. URL: https://dx.doi.org/10.1088/0029-5515/53/1/013002 (visited on 02/20/2025).

[26] Ruben Otin. "ERMES: A nodal-based finite element code for electromagnetic simulations in frequency domain". In: *Computer Physics Communications* 184.11 (Nov. 2013), pp. 2588–2595. URL: https://www.sciencedirect.com/science/article/pii/S001046551300204X (visited on 02/20/2025).

[27] Ruben Otin. "ERMES 20.0: Open-source finite element tool for computational electromagnetics in the frequency domain". In: *Computer Physics Communications* 310 (May 2025), p. 109521. URL: https://www.sciencedirect.com/science/article/pii/S0010465525000244 (visited on 02/20/2025).

[28] M. Jucker et al. "Integrated modeling for ion cyclotron resonant heating in toroidal systems". In: *Computer Physics Communications* 182.4 (Apr. 2011), pp. 912–925. URL: https://www.sciencedirect.com/science/article/pii/S0010465510005217 (visited on 02/20/2025).

[29] L.-G. Eriksson, T. Hellsten, and U. Willen. "Comparison of time dependent simulations with experiments in ion cyclotron heated plasmas". en. In: *Nuclear Fusion* 33.7 (July 1993), p. 1037. URL: https://dx.doi.org/10.1088/0029-5515/33/7/I07 (visited on 02/20/2025).

[30] E. F. Jaeger et al. “All-orders spectral calculation of radio-frequency heating in two-dimensional toroidal plasmas”. In: *Physics of Plasmas* 8.5 (May 2001), pp. 1573–1583. URL: https://doi.org/10.1063/1.1359516 (visited on 02/20/2025).

[31] Pablos Vallejos. “Modeling RF waves in hot plasmas using the finite element method and wavelet decomposition: Theory and applications for ion cyclotron resonance heating in toroidal plasmas”. English. Doctoral thesis. Stockholm: KTH, 2019. URL: https://kth.diva-portal.org/smash/get/diva2:1377064/FULLTEXT01.pdf.

[32] Dani Gallart Escolà. “Computational analysis of ion cyclotron resonance frequency heating for JET experiments”. eng. Accepted: 2020-09-06T00:01:26Z Publication Title: TDX (Tesis Doctorals en Xarxa). Doctoral thesis. Universitat Politècnica de Catalunya, Sept. 2019. URL: https://upcommons.upc.edu/handle/2117/328426 (visited on 02/20/2025).

[33] Tomás Bensadón Oliart. “Analysis of ICRF heating schemes for tokamaks using predictive integrated plasma modelling”. eng. Accepted: 2025-02-13T19:31:06Z Publication Title: TDX (Tesis Doctorals en Xarxa). Doctoral thesis. Universitat Politècnica de Catalunya, July 2024. URL: https://upcommons.upc.edu/handle/2117/424235 (visited on 02/20/2025).

[34] J Jacquot et al. “2D and 3D modeling of wave propagation in cold magnetized plasma near the Tore Supra ICRH antenna relying on the perfecly matched layer technique”. en. In: *Plasma Physics and Controlled Fusion* 55.11 (Oct. 2013). Publisher: IOP Publishing, p. 115004. URL: https://dx.doi.org/10.1088/0741-3335/55/11/115004 (visited on 02/20/2025).

[35] S. Shiraiwa et al. “Plasma wave simulation based on a versatile finite element method solvera)”. In: *Physics of Plasmas* 17.5 (May 2010), p. 056119. URL: https://doi.org/10.1063/1.3396371 (visited on 02/20/2025).

[36] V. Badalassi et al. “FERMI: Fusion Energy Reactor Models Integrator”. In: *Fusion Science and Technology* 79.3 (Apr. 2023). Publisher: American Nuclear Society, pp. 345–379. URL: https://doi.org/10.1080/15361055.2022.2151818 (visited on 02/26/2025).

[37] Pau Manyer Fuertes. “EQUILI module in ALYA: a free-boundary GradShafranov equation solver using CutFEM”. English. MA thesis. Barcelona: Universitat Politècnica de Catalunya, Oct. 2024. URL: https://fusion.bsc.es/wp-content/uploads/Pau_MScThesis_2024.pdf.

[38] A. Hrennikoff. “Solution of Problems of Elasticity by the Framework Method”. In: *Journal of Applied Mechanics* 8.4 (Mar. 2021), A169–A175. URL: https://doi.org/10.1115/1.4009129 (visited on 02/20/2025).

[39] R. Courant. “Variational methods for the solution of problems of equilibrium and vibrations”. en. In: *Bulletin of the American Mathematical Society* 49.1 (1943), pp. 1–23. URL: https://www.ams.org/bull/1943-49-01/S0002-9904-1943-07818-4/ (visited on 02/20/2025).

[40] Jian-Ming Jin. *The Finite Element Method in Electromagnetics*. en. John Wiley & Sons, Feb. 2015.

[41] M.J. Mantsinen et al. “Experiments in high-performance JET plasmas in preparation of second harmonic ICRF heating of tritium in ITER”. en. In: *Nuclear Fusion* 63.11 (Oct. 2023). Publisher: IOP Publishing, p. 112015. URL: `https://dx.doi.org/10.1088/1741-4326/aceb08` (visited on 02/21/2025).